

# Crystal Structure of the FERM Domain of Focal Adhesion Kinase\*

Received for publication, August 19, 2005, and in revised form, October 2, 2005 Published, JBC Papers in Press, October 12, 2005, DOI 10.1074/jbc.M509188200

Derek F. J. Ceccarelli<sup>‡§1</sup>, Hyun Kyu Song<sup>¶</sup>, Florence Poy<sup>‡</sup>, Michael D. Schaller<sup>||\*\*</sup>, and Michael J. Eck<sup>‡§2</sup>

From the <sup>‡</sup>Department of Cancer Biology, Dana-Farber Cancer Institute, Boston, Massachusetts 02115, the <sup>§</sup>Department of Biological Chemistry and Molecular Pharmacology, Harvard Medical School, Boston, Massachusetts 02115, the <sup>¶</sup>School of Life Sciences and Biotechnology, Korea University, Seoul 136-701, South Korea, the <sup>||</sup>Department of Cell and Developmental Biology, University of North Carolina and the <sup>\*\*</sup>Lineberger Comprehensive Cancer Center, Chapel Hill, North Carolina 27599-7090

Focal adhesion kinase (FAK) is a non-receptor tyrosine kinase that localizes to focal adhesions in adherent cells. Through phosphorylation of proteins assembled at the cytoplasmic tails of integrins, FAK promotes signaling events that modulate cellular growth, survival, and migration. The amino-terminal region of FAK contains a region of sequence homology with band 4.1 and ezrin/radixin/moesin (ERM) proteins termed a FERM domain. FERM domains are found in a variety of signaling and cytoskeletal proteins and are thought to mediate intermolecular interactions with partner proteins and phospholipids at the plasma membrane and intramolecular regulatory interactions. Here we report two crystal structures of an NH<sub>2</sub>-terminal fragment of avian FAK containing the FERM domain and a portion of the regulatory linker that connects the FERM and kinase domains. The tertiary folds of the three subdomains (F1, F2, and F3) are similar to those of known FERM structures despite low sequence conservation. Differences in the sequence and relative orientation of the F3 subdomain alters the nature of the interdomain interface, and the phosphoinositide binding site found in ERM family FERM domains is not present in FAK. A putative protein interaction site on the F3 lobe is masked by the proximal region of the linker. Additionally, in one structure the adjacent Src SH3 and SH2 binding sites in the linker associate with the surfaces of the F3 and F1 lobes, respectively. These structural features suggest the possibility that protein interactions of the FAK FERM domain can be regulated by binding of Src kinases to the linker segment.

The adhesion of cells to the extracellular matrix is mediated by the integrin family of cell surface receptors (1). Extracellular matrix engagement triggers conformational changes and clustering of integrins leading to the remodeling of protein complexes at focal adhesions (2). These intracellular complexes contain actin-cytoskeletal proteins and signaling molecules that regulate a number of processes including cell migration, proliferation, and differentiation (3). Focal adhesion kinase (FAK)<sup>3</sup>

is present at focal adhesions and becomes both tyrosine-phosphorylated and activated in response to integrin signaling (4–6). As a potential mediator of integrin signaling, it is important to understand how FAK is activated and regulated.

FAK and the related tyrosine kinase Pyk2 (also referred to as CAK- $\beta$ , RAFTK, or CADTK) comprise a subfamily of non-receptor protein-tyrosine kinases defined by a central tyrosine kinase domain flanked by an amino-terminal FERM domain and a carboxyl-terminal domain. The latter domain contains a proline-rich region that interacts with other signaling molecules and a distal focal adhesion targeting domain (Fig. 1A). Autophosphorylation of FAK at Tyr<sup>397</sup> within a linker region between the FERM and kinase domain creates a binding site for SH2-containing proteins such as Src family kinases, the p85 subunit of phosphatidylinositol 3-kinase, and Grb7 (7–11). An adjacent RXXPPXP motif serves as a binding site for the Src family SH3 domain and contributes to the efficient recruitment of Src family kinases to FAK (12, 13). Subsequent phosphorylation of tyrosines (Tyr<sup>576</sup> and Tyr<sup>577</sup>) within the kinase domain of FAK by the associated Src family kinase leads to the formation of an active signaling complex (14). Through phosphorylation of additional proteins assembled at the cytoplasmic tails of integrins, FAK and Src promote signaling events that modulate cellular growth, survival, and migration (6, 15, 16).

The amino terminus of FAK and Pyk2 share a region of homology with membrane-cytoskeletal linker proteins ezrin, radixin, and moesin (referred to collectively as ERM proteins) (17). The band 4.1 and ERM homology domain (FERM domain) is a module of ~300 amino acids found in a number of proteins that are membrane targeted (18). FERM domains of ERM proteins interact directly with the cytoplasmic regions of transmembrane receptors (19–21). In addition, association of the FERM domain with the phosphoinositide phosphatidylinositol 4,5-P<sub>2</sub> has been demonstrated both structurally and with vesicle co-sedimentation (22–24). Mutagenesis of the basic residues within the FERM domain that mediate the phosphoinositide interaction alters the subcellular distribution of the protein (24, 25). These findings suggest that both protein-protein and protein-lipid interactions may be responsible for the efficient localization of FERM-containing proteins to membrane targets.

In addition to a general role as a membrane localization module, the FERM domain may serve additional regulatory functions. Among the 518 protein kinases annotated within the human genome, FERM domains are not a common accessory domain and are only found within FAK and Janus kinase families (26). The association of Janus kinases with the cytoplasmic tails of cytokine receptors is dependent on the FERM domain (27–30). Mutations in the Janus kinase 3 FERM domain inhibit receptor binding and may abrogate kinase activity (31).

To date, several interactions involving the FERM domain of FAK have been described including those with the cytoplasmic tails of inte-

\* This work was supported in part by National Institutes of Health Grants CA080942 and HL48675. The costs of publication of this article were defrayed in part by the payment of page charges. This article must therefore be hereby marked "advertisement" in accordance with 18 U.S.C. Section 1734 solely to indicate this fact.

The atomic coordinates and structure factors (codes 2AEH and 2AL6 for FAK<sup>399</sup> and FAK<sup>405</sup>) have been deposited in the Protein Data Bank, Research Collaboratory for Structural Bioinformatics, Rutgers University, New Brunswick, NJ (<http://www.rcsb.org/>).

<sup>1</sup> Present address: Samuel Lunenfeld Research Institute, 600 University Ave., Mount Sinai Hospital, Toronto M5G 1X5, Canada.

<sup>2</sup> Recipient of a Scholar award from the Leukemia and Lymphoma Society. To whom correspondence should be addressed: SM1036, 44 Binney St., Boston, MA 02115. Tel.: 617-632-5860; Fax: 617-632-4393; E-mail: eck@red.dfci.harvard.edu.

<sup>3</sup> The abbreviations used are: FAK, focal adhesion kinase; SH2, Src homology domain 2; ERM, ezrin/radixin/moesin; ICAM-2, intercellular adhesion molecule 2; SeMet, selenomethionine; r.m.s., root mean square.

grins, the pleckstrin homology domain of the Tec-family kinase Etk, and the FERM domain of ezrin (32–35). Association with activated growth factor receptors and the promotion of cell migration in response to growth factor signaling is dependent on an intact FERM domain of FAK (36). Immunolocalization experiments have suggested that the FERM domain of FAK is sufficient for localization to membrane substructures such as at the leading edge of lamellipodia and cell-cell junctions, and although not directly responsible for focal adhesion targeting, can modulate the localization of the protein (37, 38). Finally, a direct interaction between the FERM and kinase domains of FAK may regulate the activity of the kinase (39–42). Interestingly, sequences in the F2 subdomain of the FAK FERM domain play a role in activation of FAK signaling following cell adhesion (40). The physical nature of these interactions remains to be elucidated.

To better understand the function of the FERM domain of FAK, and as a starting point for dissecting its inter- and intramolecular interactions, we have determined its structure in two crystal forms at resolutions of 2.5 Å and 2.35 Å. The tri-lobed architecture of ERM family FERM domains is preserved in FAK (22, 43–47), but a unique orientation of the F3 subdomain alters the global conformation of the domain as compared with all previously studied FERM domains. The structures show that the phosphatidylinositol 4,5- $P_2$  binding site found in ERM family FERM domains is not preserved in FAK. Additionally, the structures reveal that the FERM-kinase linker segment masks a potential protein interaction site on the F3 lobe; the corresponding site in the talin and radixin FERM domains has been shown to bind the cytoplasmic tails of  $\beta$  integrins and ICAM-2, respectively (21, 48). We hypothesize that this masking interaction could be released by binding of Src family proteins to their adjacent docking sites in the linker.

## EXPERIMENTAL PROCEDURES

**Materials**—Restriction and modifying enzymes were purchased from New England Biolabs. Oligonucleotides were from Sigma; B834 *Escherichia coli* cells were from Novagen. Seleno-L-methionine was from Sigma; metal chelating, ion exchange, and gel filtration columns were from Amersham Biosciences.

**Protein Expression and Purification**—The FERM domain of avian FAK was amplified by PCR from cDNA (Swiss-Prot accession number Q00944). DNA fragments encoding amino acids 1–405, 31–405, and 31–399 were each ligated into a modified pET vector containing an amino-terminal His<sub>6</sub> tag with a tobacco etch virus cleavage site and confirmed by DNA sequencing. The expression of recombinant protein in *E. coli* BL21(DE3) cells was induced at an optical density ( $A_{600}$ ) of 0.8 by the addition of 0.2 mM isopropyl  $\beta$ -D-thiogalactopyranoside and grown for an additional 12–16 h at 18 °C. The cells were harvested and the pellets were stored frozen at –70 °C. Cell pellets were thawed in buffer A (20 mM Tris, pH 8.0, 200 mM NaCl, 5 mM imidazole, 5 mM  $\beta$ -mercaptoethanol) with the addition of 1 mM phenylmethylsulfonyl fluoride, 10  $\mu$ g/ml leupeptin, 1 mM benzamide, 10 mg/ml lysozyme, and 1 mg/ml DNase. Cell membranes were disrupted by sonication on ice and supernatants obtained following a 30-min centrifugation at 50,000  $\times g$  were loaded onto a Ni-chelating column. Protein was eluted with buffer A containing 200 mM imidazole. FERM domain-containing fractions were pooled and the His<sub>6</sub> tag was cleaved by incubation with 1  $\mu$ g of tobacco etch virus protease per mg of protein overnight at 4 °C. The concentration of NaCl was reduced to 50 mM by dilution, and the protein was loaded onto a HiTrap Q column and eluted with buffer A containing 500 mM NaCl. The FERM domain was concentrated and loaded onto a Superdex 75 size exclusion column previously equilibrated in buffer A containing 100 mM NaCl. The eluted FERM domain

of FAK was greater than 95% pure as estimated by SDS-PAGE and was concentrated to 6–10 mg/ml and stored at –70 °C.

Selenomethionine (SeMet)-substituted protein was prepared using the methionine auxotroph B834(DE3) strain. Cells were grown in M9 minimal media supplemented with SeMet (40  $\mu$ g/ml). The subsequent steps for SeMet-labeled FERM domain proceeded as described for the native protein.

**Crystallization and Data Collection**—Protein crystals of FAK<sup>399</sup> (residues 31–399 of avian FAK) were obtained by the hanging drop method using 6–10 mg/ml protein mixed in a 1:1 volume ratio with precipitation solution containing 100 mM Tris, pH 8.0, 16–22% polyethylene glycol 4000, 20% glycerol, 200 mM NaCl, 100 mM CsCl, 10 mM dithiothreitol. Crystals grew over 1–2 weeks at room temperature reaching maximum dimensions of 40  $\times$  100  $\times$  20  $\mu$ m. Diffraction data were recorded to 2.5-Å resolution from a single, frozen native crystal with a monoclinic space group, P2<sub>1</sub> and unit cell parameters  $a = 44.2$ ,  $b = 146.2$ ,  $c = 68.9$  Å,  $\beta = 96.4^\circ$ . Multiple anomalous diffraction data on a single, frozen, SeMet-derivatized FAK<sup>399</sup> crystal was collected at the NSLS X12C beamline to 2.9-Å resolution (see Table 1 for details). Crystals of FAK<sup>405</sup> (residues 31–405) were grown in 22.5% polyethylene glycol 4000, 0.1 M citrate, pH 5.5, 0.2 M ammonium acetate, 20% glycerol, and in the presence of 1:2 molar ratio of inositol (1,4,5) $P_3$ . The phosphoinositide head group did not affect crystallization and is not present in the crystal structure. Diffraction data from a single frozen crystal with an orthorhombic space group (unit cell  $a = 50.54$ ,  $b = 123.99$ ,  $c = 133.93$  Å) was collected at APS (14-ID-B) to 2.35-Å maximum resolution.

**Structure Determination**—The program SOLVE was used to determine the position of 10 selenium atoms from two copies of the FERM domain in the asymmetric unit in the FAK<sup>399</sup> structure. The initial electron density map was improved by solvent flattening and phase-extension to 2.5-Å resolution using program DM (49). A partial model was built automatically using the program ARP/wARP (50). The structure was completed and refined with several rounds of manual rebuilding using the program O and atomic refinement with CNS. The model was assessed using PROCHECK (51) and waters were added by CNS. The refined model contains residues 33–363 of FAK, whereas residues 31–32 and 364–399 were not visible in the electron density maps and presumed to be disordered.

The structure of FAK<sup>405</sup> was phased by molecular replacement using the previously determined FAK<sup>399</sup> FERM structure as the search model and the program Phaser (52). Difference electron density maps revealed that the ordered portion of one of the two molecules in the asymmetric unit extended to residue 375, and also revealed density corresponding to residues 394–403 and 394–401 in the linker regions of the two molecules. These regions were built and the FAK<sup>405</sup> structure was refined as described above for the FAK<sup>399</sup> structure.

## RESULTS

**Domain Mapping, Crystallization, and Structure Determination**—The amino-terminal fragment of FAK (residues 1–405) containing the predicted FERM domain and autophosphorylation site Tyr<sup>397</sup> was expressed in *E. coli* and purified. Limited proteolysis with the protease trypsin and amino-terminal sequencing of the resulting polypeptide identified a cleavage event that removed the NH<sub>2</sub>-terminal 28 residues of FAK (data not shown). Analysis of the FERM region of FAK and PYK2 from a number of species revealed that sequence conservation initiated with Arg<sup>35</sup> (numbering refers to avian FAK). A truncated protein containing residues 31–399 (referred to here as FAK<sup>399</sup>) was generated and produced monoclinic crystals that diffracted x-rays to better than 2.5-Å

**TABLE 1**  
Data collection and refinement statistics for FAK FERM domain

	31–399 SeMet (multiple anomalous diffraction)				
	31–399	Inflection	Peak	Remote	31–405
<b>Data collection</b>					
Wavelength (Å)	0.97897	0.9796	0.9793	0.95004	1.12714
Resolution (Å) (outer shell) <sup>a</sup>	30–2.5 (2.57–2.50)	30–2.8 (2.9–2.8)	30–2.8 (2.9–2.8)	30–2.9 (3.0–2.9)	30–2.35 (2.45–2.35)
Space group	P2 <sub>1</sub>	P2 <sub>1</sub>	P2 <sub>1</sub>	P2 <sub>1</sub>	P2 <sub>1</sub> 2 <sub>1</sub> 2 <sub>1</sub>
Total reflections	139,555	147,041	147,592	73,310	274,336
Unique reflections	29,897	21,456	21,509	19,210	35,886
Completeness (%) <sup>a</sup>	100 (100)	98.7 (97.2)	99.3 (97.9)	99.4 (99.6)	99.7 (99.9)
I/σ <sup>a</sup>	22.5 (2.7)	24.6 (2.6)	25.3 (3.0)	15.7 (2.1)	13.7 (2.7)
R <sub>merge</sub> (%) <sup>a,b</sup>	0.073 (0.50)	0.09 (0.76)	0.088 (0.68)	0.111 (0.79)	0.038 (0.28)
<b>Figure of merit<sup>c</sup> before/after DM</b>	0.39 for 20–2.9 Å/0.64 for 39–2.5 Å				
<b>Refinement</b>					
Resolution range (Å)	20–2.5				30–2.35
Reflections (free/test)	27,037/1,405				34,091/1,795
R <sub>work</sub> /R <sub>free</sub> (%) <sup>d</sup>	19.6/24.9				21.0/25.2
Protein	5,369				5,465
Water	243				155
r.m.s. bond length (Å)	0.0058				0.0067
r.m.s. bond angles (°)	1.16				1.15
<b>Average B-value (Å<sup>2</sup>)</b>					
Protein	50.6				50.6
Water	48.7				47.8

<sup>a</sup> Values in parentheses are for reflections in the highest resolution bin.

<sup>b</sup>  $R_{\text{merge}} = \sum_i |I(h_i) - \langle I(h) \rangle| / \sum_i I(h_i)$ , where  $I(h_i)$  is the intensity of the  $i^{\text{th}}$  measurement of  $h$  and  $\langle I(h) \rangle$  is the corresponding average value for all  $i$  measurements.

<sup>c</sup> Figure of merit =  $|\sum P(\alpha) e^{i\alpha P} / \sum P(\alpha)|$ , where  $P(\alpha)$  is the phase probability distribution and  $\alpha$  is the phase.

<sup>d</sup>  $R_{\text{work}}$  and  $R_{\text{free}} = \sum ||F_o| - |F_c|| / \sum |F_o|$  for the working set and test set (5%) of reflections.

resolution. The FAK<sup>399</sup> structure was determined by multiwavelength anomalous diffraction methods using SeMet-substituted protein. We also obtained crystals with a longer construct spanning residues 31–405 (FAK<sup>405</sup>); this structure was determined by molecular replacement using the FAK<sup>399</sup> structure as a model. The two structures are essentially the same; the only notable exception is that in the FAK<sup>405</sup> structure, we observe electron density for a portion of the FERM-kinase linker corresponding to the Src SH3 binding site (residues 364 to 375) and for the segment containing the Tyr<sup>397</sup> autophosphorylation site (residues 394–403). These segments are not ordered or completely present in the FAK<sup>399</sup> crystals. Our description of the structure below is based upon the FAK<sup>399</sup> crystals, but we refer explicitly to FAK<sup>399</sup> or FAK<sup>405</sup> as necessary for correctness and clarity.

The FAK<sup>399</sup> protein crystallized in monoclinic space group P2<sub>1</sub> with two molecules in the asymmetric unit. The final model contains two molecules of the FERM domain and 243 water molecules and has been refined to an  $R$  value of 19.6% ( $R_{\text{free}} = 24.9\%$ ) at 2.5-Å resolution with excellent stereochemistry (Table 1). The first 2 residues (Gly<sup>31</sup>-Ala<sup>32</sup>) and the COOH-terminal 37 residues (Lys<sup>364</sup>-Glu<sup>399</sup>) in each molecule are not visible in the electron density; this disordered region includes the Src SH3 binding site (Arg<sup>368</sup>-Pro<sup>374</sup>) and the Tyr<sup>397</sup> phosphorylation site. FAK<sup>405</sup> protein crystallized in the orthorhombic space group P2<sub>1</sub>2<sub>1</sub>2<sub>1</sub>, also with two molecules in the asymmetric unit. Residues Ser<sup>307</sup>-Arg<sup>312</sup>, Leu<sup>376</sup>-Glu<sup>393</sup>, and Glu<sup>404</sup>-Asp<sup>405</sup> were not observed in the electron density and are not included in the final model. The FAK<sup>405</sup> structure has been refined to an  $R$  value of 21.0% ( $R_{\text{free}} = 25.2\%$ ) with good stereochemistry (Table 1 and “Experimental Procedures”).

**Structure of the FAK FERM Domain**—The FAK structure reveals the three-lobed architecture characteristic of the archetypal FERM domains of ERM family members ezrin (47), radixin (22), and moesin (43) (Fig. 1B). The three subdomains (labeled F1, F2, and F3) intimately associate with one another to form a compact structure with the overall shape of a cloverleaf. Each of the three lobes of the FERM domain bears striking similarity to otherwise unrelated single-domain protein structures as previously noted (43). The F1 lobe spans residues 33–127 and exhibits a ubiquitin-like fold (53) consisting of a five-stranded  $\beta$ -sheet

capped by an  $\alpha$ -helix. The F2 subdomain (residues 128–253) is all  $\alpha$ -helical and contains a core 4-helix bundle similar to that found in the acyl-CoA-binding protein (54). The F3 lobe (residues 254–352) is a  $\beta$ -sandwich capped by a COOH-terminal  $\alpha$ -helix that very closely resembles a pleckstrin homology domain. The pleckstrin homology domain shares the same three-dimensional fold with other modular signaling domains including phosphotyrosine binding and EVH1 domains in addition to the F3 lobe of the FERM domain (55). It has evolved distinct binding sites for diverse protein and phospholipid ligands (56). Both phosphotyrosine binding domains and the F3 lobe of some FERM domains bind peptide ligands in a groove formed between one edge of the  $\beta$ -sandwich and the COOH-terminal  $\alpha$ -helix. Interestingly, this groove is occupied in the FAK FERM domain by residues just COOH-terminal to the FERM domain in the FERM-kinase linker segment (Fig. 4). This interaction is observed in both FAK<sup>399</sup> and FAK<sup>405</sup> and is discussed more fully in a following section.

The two protein molecules in the asymmetric unit are quite similar. They superimpose with a root mean square (r.m.s.) deviation of 0.9 Å over 330 amino acids. The only significant structural deviations in the two molecules are found in loop regions (the loop connecting  $\alpha 2$  and  $\alpha 3$  in the F2 lobe, the loop between strands  $\beta 3$  and  $\beta 4$ , and the loop between strands  $\beta 5$  and  $\beta 6$  loop in the F3 lobe). Similarly, the FAK<sup>405</sup> structure superimposes well with that of FAK<sup>399</sup> (r.m.s. deviation of 1.2 Å for 324 equivalent residues). Both structures reveal a similar non-crystallographic dimer interface, but the contact between the two molecules is small (it buries  $\sim 400$  Å<sup>2</sup> of surface area on each monomer) and is therefore not suggestive of a biologically relevant dimer. Also, the isolated FERM domain elutes in size-exclusion chromatography at a volume consistent with a monomeric protein (data not shown). However, FAK self-association is thought to play a role in its catalytic regulation and we cannot exclude the possibility that the FERM-FERM interaction observed in the crystal lattice is part of a larger interaction in the intact kinase.

**Comparison with the Radixin FERM**—The FAK FERM domain is rather distantly related to other FERM domains. For example, it shares only 12–15% sequence identity with ERM family members (Fig. 1C).

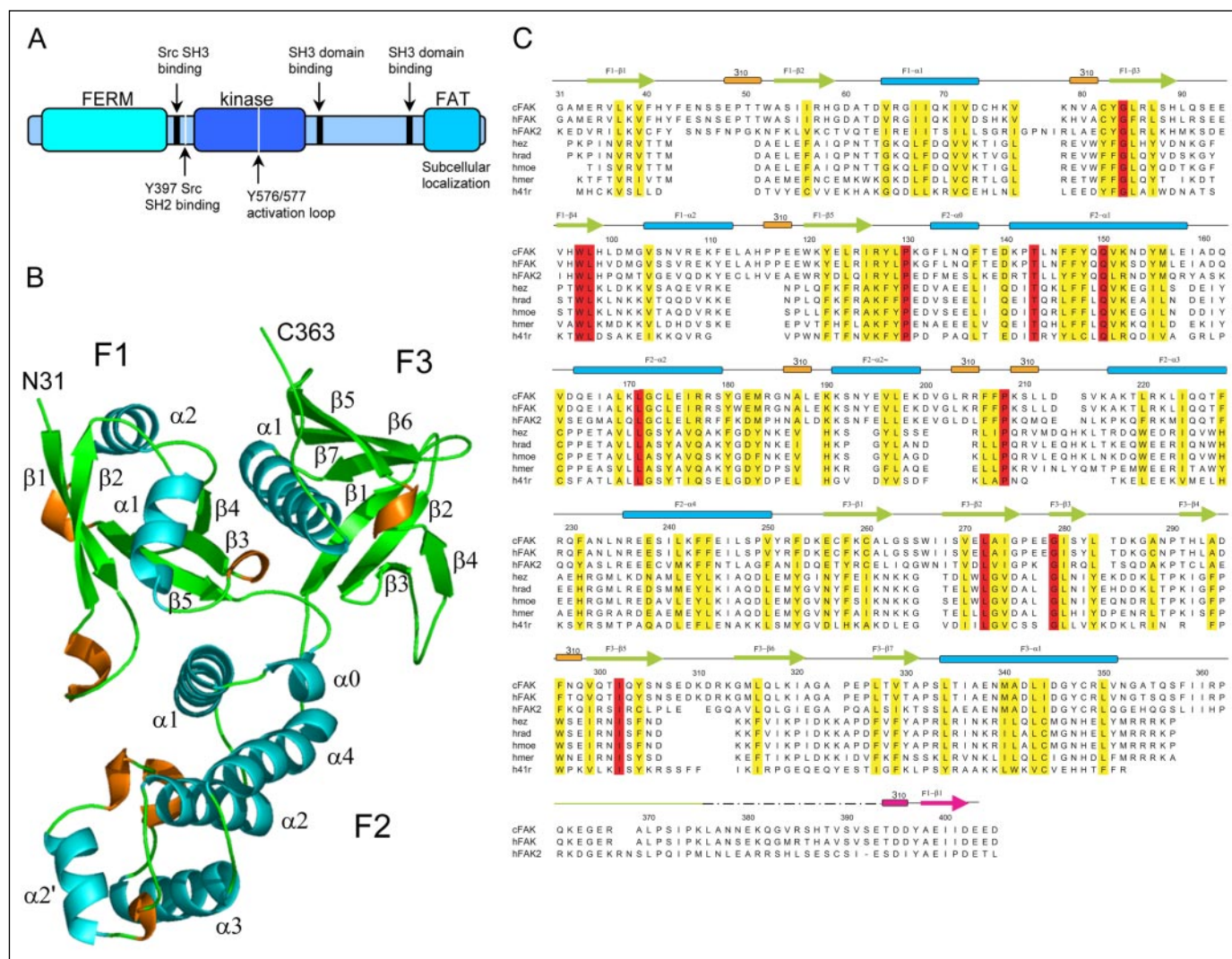


**FIGURE 1. Structure and sequence comparison of the FAK FERM domain.** *A*, schematic showing the domain organization of FAK. The FERM, tyrosine kinase, and focal adhesion targeting (FAT) domains are indicated, as are principle tyrosine phosphorylation sites and the Src SH3 binding motif in the FERM/kinase linker segment. *B*, ribbon diagram of FAK FERM domain containing amino acids 33–363. The three subdomains are labeled *F1*, *F2*, and *F3* with  $\alpha$ -helices colored cyan,  $\beta$ -strands colored green, and  $3_{10}$  helical turns in orange. Secondary structure elements are labeled as shown in the sequence alignment below. *C*, structure-based sequence alignment of FERM domains with conserved residues highlighted in yellow and identical residues in red. Avian FAK (*cFAK*), human FAK (*hFAK*), human Pyk2 (*hPYK2*), human Ezrin (*hEz*), human radixin (*hRad*), human moesin (*hMoe*), human merlin (*hMer*), and human band 4.1R (*h41R*) are shown.

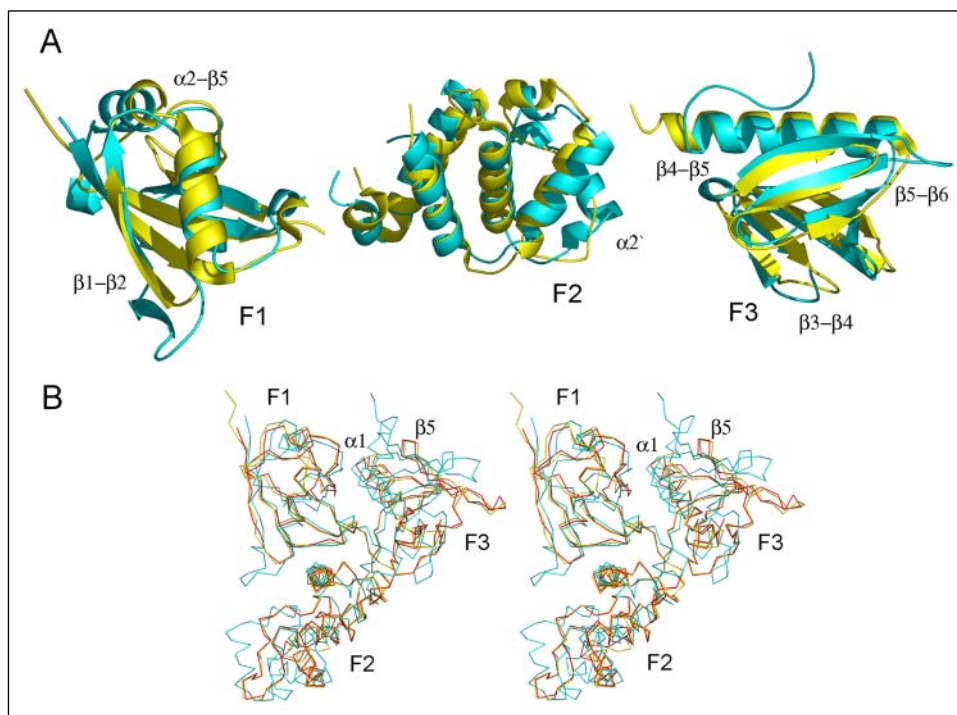
This considerable sequence divergence is reflected in significant structural changes in the FAK FERM domain as compared with other FERM domain structures studied to date. As expected, the overall fold of the FERM domain is preserved, but marked differences are observed both in the structures of the individual lobes and in their relative orientations within the domain as a whole (Fig. 2). In contrast, the FERM domains of merlin and ERM family members much more closely resemble one another (they superimpose with overall root mean square deviations on the order of 1 Å or less). We compare the FAK FERM domain with that of radixin, a well studied ERM family member.

The 64-residue core of the *F1* subdomain superimposes with that of radixin with an r.m.s. deviation of 1.4 Å (Fig. 2A). The second helix in the *F1* subdomain (*F1- $\alpha$ 2*) is approximately two turns longer in FAK than in ERM family members. Additionally, the  $\beta$ 1- $\beta$ 2 and  $\alpha$ 2- $\beta$ 5 loop regions are longer, and contain  $3_{10}$  helices not found in other FERM structures. These insertions account for the 12 additional residues within the *F1* domain of FAK as compared with the structurally aligned FERM domain of radixin (Fig. 1C). Structural similarity with the *F2* subdomain of radixin is limited to helices  $\alpha$ 1 to  $\alpha$ 4; the 78 residues in this 4-helix

core superimpose with an r.m.s. deviation of 1.6 Å. The FAK *F2* lobe includes four structural elements that are not seen in other FERM structures; these include three segments of  $3_{10}$  helix and a 9-residue helix  $\alpha$ 2', all of which are inserted between core helices  $\alpha$ 2 and  $\alpha$ 3 (Figs. 1C and 2A). The *F3* lobes of FAK and radixin superimpose with an r.m.s. deviation of 1.5 Å over 73 residues for 6 of the 7  $\beta$ -strands and the  $\alpha$ 1 helix. The relatively modest structural differences between the *F3* subdomains of FAK and radixin include a shift in the position of the  $\beta$ 3- $\beta$ 4 loop, a  $3_{10}$  helix within  $\beta$ 4- $\beta$ 5 turn in FAK, and a 7-residue insertion in the loop connecting strands  $\beta$ 5 and  $\beta$ 6.

Perhaps the most striking structural difference between the FAK FERM domain and other intact FERM structures determined to date is the relative orientation of the subdomains. In particular, the position of the *F3* lobe with respect to the *F1* and *F2* lobes is markedly different in FAK. The FAK FERM domain is shown superimposed with the structurally related radixin and merlin FERM domains in Fig. 2B. The FAK *F3* subdomain is rotated and translated such that its  $\alpha$ 1 helix is positioned 3.5–4 Å closer to the *F1* lobe and its  $\beta$ 5 strand is  $\sim$ 9 Å closer to the *F1* lobe than the equivalent regions in radixin and merlin. This difference is

**FIGURE 2. Comparison of FAK with a representative ERM family FERM domain.** *A*, the F1, F2, and F3 subdomains of avian FAK (shown in cyan) and human radixin (shown in yellow) were superimposed individually. The subdomains are highly related but notable structural differences are described in the text. *B*, superposition of the intact FERM domains of FAK (cyan), radixin (yellow), and merlin (red). The different orientation of FAK F3 with respect to the F1 and F2 lobes is apparent in comparison with the overall structural conservation between radixin and merlin characteristics of all ERM family and closely related FERM domains studied to date.



much greater than the shift described in comparison of the active and inactive-tail bound structures of moesin and ezrin (47, 57). The net effect of this rearrangement is a significant difference in the interfaces of F3 with both F1 and F2 as compared with other intact FERM structures. The F3 lobe is less intimately associated with the F2 lobe in FAK (a buried surface area of 749 Å<sup>2</sup> as compared with 990 Å<sup>2</sup> of contact in radixin). In contrast, the F1–F3 interface is more intimate (compare 1207 Å<sup>2</sup> buried in FAK with 1004 Å<sup>2</sup> in radixin). Interacting residues between the F1 and F3 domains of FAK include His<sup>99</sup> with Glu<sup>338</sup>, Arg<sup>127</sup> with Asp<sup>342</sup>, and Asn<sup>339</sup> with Val<sup>195</sup> and Trp<sup>97</sup>. This novel positioning of F3 against F1 is the same in the two independent FAK molecules in the crystallographic asymmetric unit and also observed in the FAK<sup>405</sup> structure, which has different crystal packing contacts.

The divergent structure of the FAK FERM domain also indicates a divergence in function. The FERM domains of ERM proteins bind phosphoinositide phosphatidylinositol 4,5-P<sub>2</sub>; this interaction is important for localization of the ERM proteins in cells (24). The radixin FERM domain has been crystallized in complex with inositol 1,4,5-trisphosphate (the soluble head group of phosphatidylinositol 4,5-P<sub>2</sub>) (22). The IP<sub>3</sub> head group binds radixin in a shallow, basic cleft between the F1 and F3 domains (Fig. 3*B*). The FAK FERM domain clearly cannot bind phosphoinositides in the analogous position (Fig. 3, *A* and *C*). In FAK, the F1–F3 cleft is different in both structure and amino acid composition. The interface between the F1 and F3 domains of FAK is narrow relative to other FERM structures because of the divergent position of the F3 lobe as described above. Additionally, the presence of acidic residues and the lack of basic residues within this cleft is expected to preclude phosphoinositide coordination at this site in the FERM domain of FAK (Fig. 3, *C* and *D*).

**The FERM-Kinase Linker Segment**—In human FAK, the FERM domain ends at residue 352, and the kinase domain begins at approximately residue 415 (58). The intervening 60-residue linker segment is important for regulation of FAK function, as it contains the Tyr<sup>397</sup> phosphorylation site (which when phosphorylated is bound by the Src SH2 domain) and also the binding site for the Src SH3 domain. The linker is

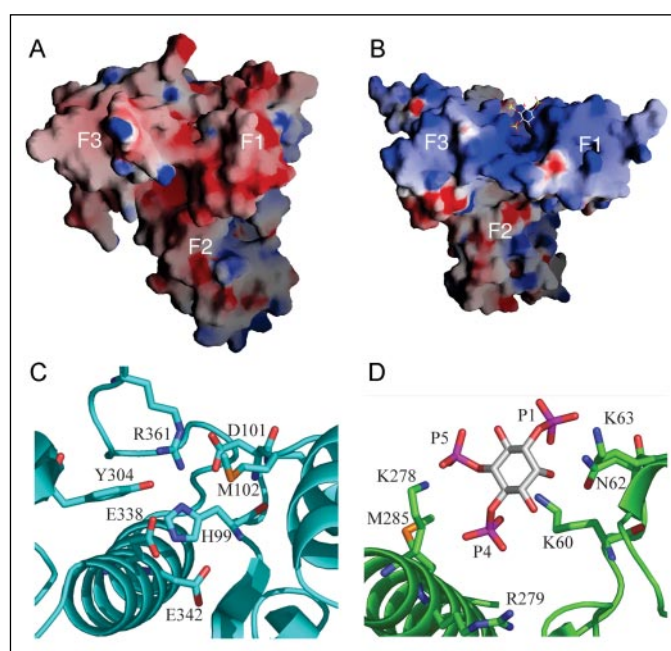


**FIGURE 3. Electrostatic surface representations of the FAK (A) and radixin (B) FERM domains and detail of the F1–F3 cleft in FAK (C) and radixin (D).** The electrostatic surfaces are shaded *blue* in basic regions and *red* in acidic regions. In the radixin structure (Protein Data Bank code 1GC6), inositol 1,4,5-trisphosphate (IP<sub>3</sub>) is bound in the center of a basic cleft between the F1 and F3 lobes, where it is coordinated in part by the side chains of three lysine residues (*panel D*). Note that this basic cleft is not present in the FAK FERM domain (*panels A* and *C*), and that the proximal portion of the FERM-kinase linker segment (the residues flanking Arg<sup>361</sup>) binds in this region (*panel C*).

largely disordered in FAK<sup>399</sup>, however, in both the FAK<sup>399</sup> and FAK<sup>405</sup> structures the first 10 residues of the linker bind in the cleft between the F1 and F3 lobes and in the putative peptide recognition groove on the F3 lobe (Fig. 4). In the longer FAK<sup>405</sup> structure, the ordered region extends to Lys<sup>375</sup> and encompasses the Src SH3 docking site. Additionally, a discontinuous segment of clear density is observed for residues 394–

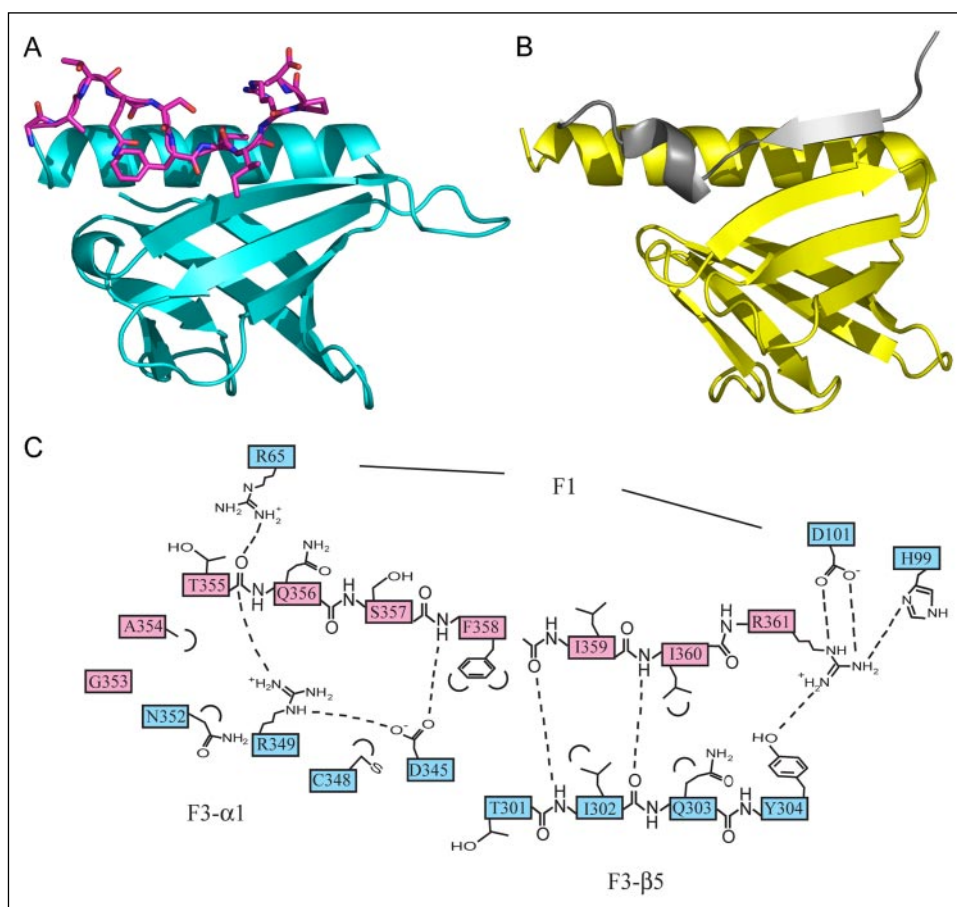


**FIGURE 4. Detailed view of the F3 lobe highlighting the linker interaction.** A, ribbon diagram of the FAK F3 lobe with the proximal portion of the linker shown in stick form and colored magenta. The details of this interaction are shown schematically in panel C. B, the radixin F3 lobe (yellow) bound to a peptide representing the cytoplasmic tail of ICAM-2 (gray). C, schematic detailing the interactions of the linker with the putative ligand binding groove on the F3 lobe. Linker residues are indicated in magenta, FERM domain residues in cyan. Dashed lines indicate hydrogen bond interactions and semicircles indicate hydrophobic interactions. Note that the linker also contacts the F1 lobe as indicated.

403 of the FERM-kinase linker; this segment encompasses the Tyr<sup>397</sup> site (Fig. 5).

Just COOH-terminal to the  $\alpha 1$  helix of F3, the polypeptide chain turns back into the F1–F3 cleft, and makes numerous interactions with both the F1 lobe and the F3 binding groove (Fig. 4, A and C). Contacts with the F1 lobe include a salt-bridge hydrogen bond network involving Arg<sup>361</sup> in the linker and the side chains of Asp<sup>101</sup> and His<sup>89</sup> in the F1 lobe, and also a hydrogen bond between the carbonyl of Thr<sup>355</sup> and the side chain of Arg<sup>65</sup> in the F1 lobe. The linker interaction with the F3 binding groove is stabilized by hydrophobic interactions of Phe<sup>358</sup>, Ile<sup>359</sup>, and Ile<sup>360</sup> and through a parallel  $\beta$ -sheet interaction of residues Phe<sup>358</sup> to Ile<sup>360</sup> with the  $\beta 5$  strand in the F3 binding groove (Fig. 4C). In the FAK<sup>399</sup> structure, the linker region beyond Pro<sup>362</sup> no longer contacts the FERM domain. However, in one of the two molecules in the FAK<sup>405</sup> structure, the ordered region extends through the Src SH3 binding site (residues 368–375), which interacts with the surface of the F3 lobe (Fig. 5, A and B). The RALPSIP sequence (the key residues of the RXXPPXP Src SH3 binding motif are underlined) adopts a polyproline type II helical conformation and packs against the exposed  $\beta$ -sheet of the F3 lobe. Contacts with the F3 subdomain include 5 backbone-mediated hydrogen bond interactions including two with the side chains of Gln<sup>303</sup> and Gln<sup>317</sup>, and hydrophobic interactions involving Leu<sup>370</sup> and Ile<sup>373</sup> (Fig. 5B). Interestingly, polyproline motifs bind to EVH1 domains of Ena/Vasp proteins, which also share the pleckstrin homology domain fold of the F3 lobe, in a topologically similar location (59). The orientation and specific interactions of the proline motif in the present structure, however, is not the same as that observed in EVH1 complexes.

The segment containing the phosphorylation site Tyr<sup>397</sup> packs against the F1 subdomain of both FERM molecules (Fig. 5, A and C).

This polypeptide consists of residues 394–403 and forms a  $3_{10}$  helix and short  $\beta$ -strand that extends the anti-parallel  $\beta$ -sheet formed by the  $\beta 1$  and  $\beta 2$  strands of F1. This interface buries a total of 1047 Å<sup>2</sup> and comprises 7 backbone-mediated hydrogen bonds with only Thr<sup>62</sup> of F1 making a specific side chain interaction and two side chain-mediated interactions of Glu<sup>403</sup> with Ser<sup>54</sup> and His<sup>41</sup> (Fig. 5C). There are no previously identified examples of this surface of a FERM domain making a protein-protein interaction. The side chain of Tyr<sup>397</sup> is surface exposed and in close proximity to Lys<sup>70</sup>. The last ordered residue of the COOH-terminal segment, Glu<sup>403</sup>, is near Lys<sup>38</sup>, His<sup>41</sup>, His<sup>75</sup>, and the cleft region between the F1 and F2 subunits. Note that it is not possible to ascertain whether the interaction of this segment is intramolecular or whether it occurs between adjacent molecules in the crystal lattice because we do not observe density for the preceding 20 residues. Either connectivity is crystallographically plausible, but the fact that this construct is monomeric in solution suggests that the interaction is intramolecular.

## DISCUSSION

The F3 binding groove, occupied by the NH<sub>2</sub>-terminal portion of the linker segment in the present structure, is a well characterized interaction site on FERM domains. In ERM family proteins, this groove is occupied by part of the COOH-terminal actin-binding tail, which makes intramolecular interactions with the FERM domain (43). Upon activation, this autoinhibitory conformation is thought to be released, allowing interaction with the cytoplasmic tails of cognate cell-surface receptors (60). Indeed, the tail region of ICAM-2 was recently demonstrated to bind at this site in a crystal structure of radixin complexed with an ICAM-2 peptide (21). The peptide forms a  $\beta$ -sheet interaction with the  $\beta 5$  strand of the F3 lobe, thereby extending the  $\beta$ -sheet (Fig.

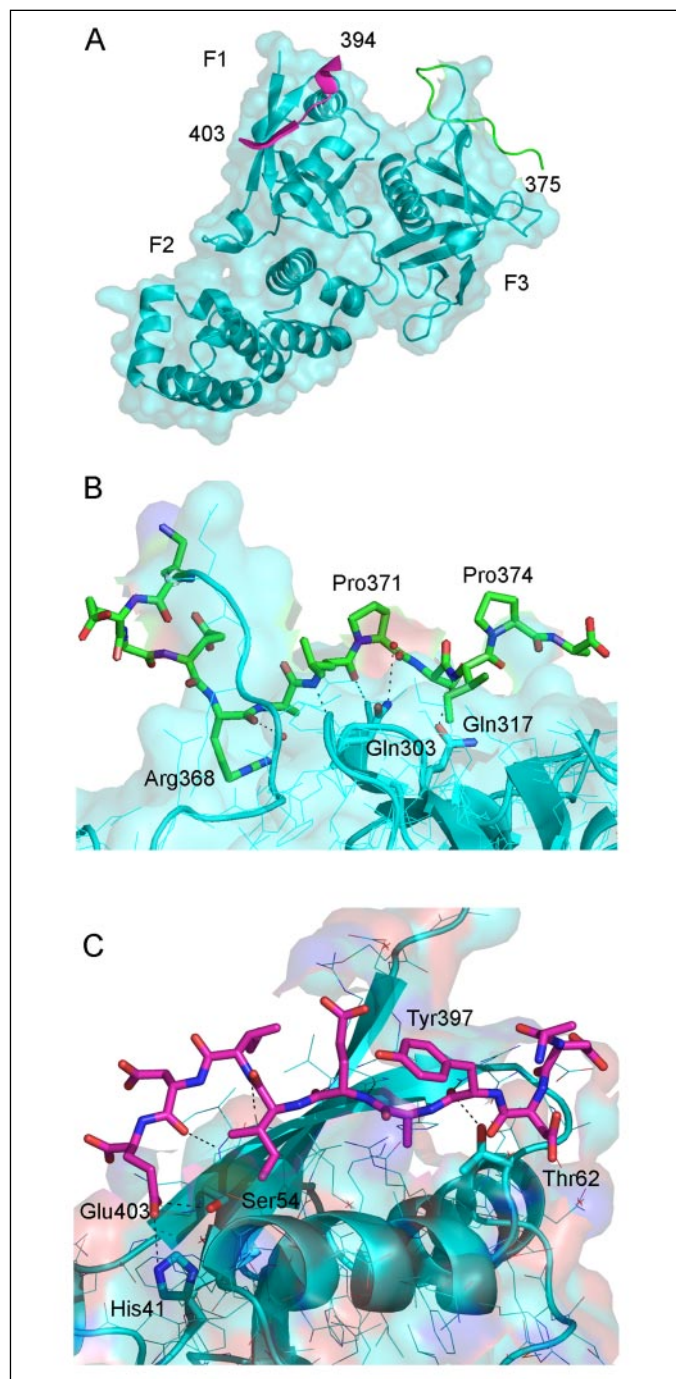


**FIGURE 5. Portions of the FERM kinase linker including the Src SH3 binding site and the Tyr<sup>397</sup> autophosphorylation site are tethered across the surface of the F1 and F3 subdomains in the FAK<sup>405</sup> structure.** *A*, ribbon and transparent surface representation of the FAK FERM domain. The Src SH3 binding site is shown in green (residues 363–375) and the Tyr<sup>397</sup>-containing segment (residues 394–403) is colored in pink. *B*, detail of the interactions between the Src SH3-binding site and the surface of F3. Hydrogen bonds between the RXPXPX motif (residues Arg<sup>368</sup> to Pro<sup>374</sup>) and the F3 lobe are indicated by dashed lines and involve the side chains of Gln<sup>303</sup> and Gln<sup>317</sup> on the F3 lobe. *C*, details of the interaction between the FAK autophosphorylation Tyr<sup>397</sup> segment and the F1 lobe. Hydrogen bonds are indicated with dashed lines and involve the side chains of Glu<sup>403</sup> with His<sup>41</sup> and Ser<sup>54</sup> bonds. Tyr<sup>397</sup> is surface exposed and not phosphorylated in the structure.

4*B*). Additionally, the corresponding site in the talin FERM domain was observed to bind an NPXY motif in the  $\beta 3$  integrin tail (48). Interestingly, this binding site is also analogous to that bound by NPXY motif sequences on the structurally homologous phosphotyrosine binding

domain, as seen, for example, in the insulin receptor substrate-1 phosphotyrosine binding domain (61). Although the linker segment in FAK binds to the F3 lobe in the same location, its mode of binding is quite different from that in the structures noted above. The linker segment binds in the opposite orientation, thus forming a parallel rather than anti-parallel  $\beta$ -sheet interaction with strand  $\beta 5$  (Fig. 4).

The significance of the interaction of the NH<sub>2</sub>-terminal portion of the linker with the F3 lobe is unclear. It is possible that this portion of the linker segment is simply an extension of the fold of the FAK FERM domain itself, and therefore represents a structural divergence between FAK and other FERM domains. Alternatively, it is tempting to speculate that it represents a regulatory interaction, masking all or part of the binding site of an interacting protein. Like talin, FAK may associate with  $\beta$ -integrin tails. If it is a regulatory interaction, the structure suggests that it might be released by binding of a Src family protein to the SH3 and/or SH2 binding sites. Indeed, binding of a Src SH3 domain to the RALPSIP sequence would preclude its interaction with the surface of the F3 lobe and might also destabilize the interaction of the linker in the F3 groove by steric effects. The phosphorylation of Tyr<sup>397</sup> is a key regulatory event in the activation of FAK and scaffolding properties that recruit SH2-domain containing proteins such as Src family kinases, phosphatidylinositol 3'-kinases, and Grb family adaptor proteins (62). Phosphorylation and subsequent binding to the Tyr<sup>397</sup> site will also require its dissociation from the surface of the FERM domain.

Although structurally unrelated, the interactions of the linker segment with the FERM domain are reminiscent of the intramolecular interactions between the SH3 domain and the SH2 kinase linker segment in Src family kinases. It is tempting to speculate that one or both of the linker contacts may additionally participate in autoinhibitory interactions with the kinase, in analogy with Src kinases where the SH3 and linker together bind the N-lobe of the kinase (63). In FAK, association of SH2-containing proteins may be an important step in the activation of the kinase by facilitating disassembly of the FERM-linker and/or FERM/kinase intramolecular interactions. In loose analogy with Src kinases, phosphorylation of Tyr<sup>397</sup> and subsequent recruitment of a Src family kinase to the linker segment might be expected to stabilize an open and active conformation of FAK. The present structure will facilitate mutagenesis studies designed to test these possibilities and to further dissect the intramolecular interaction of the FERM domain with the kinase domain.

## REFERENCES

- Giancotti, F. G., and Ruoslahti, E. (1999) *Science* **285**, 1028–1032
- Xiong, W.-C., and Mei, L. (2003) *Front. Biosci.* **8**, 676–682
- Zamir, E., and Geiger, B. (2001) *J. Cell Sci.* **114**, 3583–3590
- Schlaepfer, D. D., Hauck, C. R., and Sieg, D. J. (1999) *Prog. Biophys. Mol. Biol.* **71**, 435–478
- Schaller, M. D. (2001) *Biochim. Biophys. Acta* **1540**, 1–21
- Parsons, J. T. (2003) *J. Cell Sci.* **116**, 1409–1416
- Schaller, M., Hildebrand, J. D., Shannon, J. D., Fox, J. W., Vines, R. R., and Parsons, J. T. (1994) *Mol. Cell. Biol.* **14**, 1680–1688
- Han, D. C., and Guan, J.-L. (1999) *J. Biol. Chem.* **274**, 24425–24430
- Chen, H.-C., Appeddu, P. A., Isoda, H., and Guan, J.-L. (1996) *J. Biol. Chem.* **271**, 26329–26334
- Schlaepfer, D. D., and Hunter, T. (1996) *Mol. Cell. Biol.* **16**, 5623–5633
- Reiske, H. R., Kao, S.-C., Cary, L. A., Guan, J.-L., Lai, J.-F., and Chen, H.-C. (1999) *J. Biol. Chem.* **274**, 12361–12366
- Thomas, J. W., Ellis, B., Boerner, R. J., Knight, W. B., White, G. C., II, and Schaller, M. D. (1998) *J. Biol. Chem.* **273**, 577–583
- Hauck, C. R., Hunter, T., and Schlaepfer, D. D. (2001) *J. Biol. Chem.* **276**, 17653–17662
- Calalb, M. B., Polte, T. R., and Hanks, S. K. (1995) *Mol. Cell. Biol.* **15**, 954–963
- Playford, M. P., and Schaller, M. D. (2004) *Oncogene* **23**, 7928–7946
- Schlaepfer, D. D., Mitra, S. K., and Ilic, D. (2004) *Biochim. Biophys. Acta* **1692**, 77–102
- Girault, J.-A., Labesse, G., Mornon, J.-P., and Callebaut, I. (1999) *Trends Biochem. Sci.*

- 24, 54–57
18. Chishti, A. H. (1998) *Trends Biochem. Sci.* **23**, 281–282
  19. Hirao, M., Sato, N., Kondo, T., Yonemura, S., Monden, M., Sasaki, T., Takai, Y., Tsukita, S., and Tsukita, S. (1996) *J. Cell Biol.* **135**, 37–51
  20. Mangeat, P., Roy, C., and Martin, M. (1999) *Trends Cell Biol.* **9**, 187–192
  21. Hamada, K., Shimizu, T., Yonemura, S., Tsukita, S., Tsukita, S., and Hakoshima, T. (2003) *EMBO J.* **22**, 502–514
  22. Hamada, K., Shimizu, T., Masui, T., Tsukita, S., Tsukita, S., and Hakoshima, T. (2000) *EMBO J.* **19**, 4449–4462
  23. Niggli, V., Andreoli, C., Roy, C., and Mangeat, P. (1995) *FEBS Lett.* **376**, 172–176
  24. Barret, C., Roy, C., Montcourrier, P., Mangeat, P., and Niggli, V. (2000) *J. Cell Biol.* **151**, 1067–1079
  25. Bompard, G., Martin, M., Roy, C., Vignon, F., and Friess, G. (2003) *J. Cell Sci.* **116**, 2519–2530
  26. Manning, G., Whyte, D. B., Martinez, R., Hunter, T., and Sudarsanam, S. (2002) *Science* **298**, 1912–1934
  27. Huang, L. J.-s., Constantinescu, S. N., and Lodish, H. F. (2001) *Mol. Cell* **8**, 1327–1338
  28. Haan, C., Is'harc, H., Hermanns, H. M., Schmitz-Van de Leur, H., Kerr, I. M., Heinrich, P. C., Grotzinger, J., and Behrmann, I. (2001) *J. Biol. Chem.* **276**, 37451–37458
  29. Hilkens, C. M., Is'harc, H., Lillemeier, B. F., Strobl, B., Bates, P. A., Behrmann, I., and Kerr, I. M. (2001) *FEBS Lett.* **505**, 87–91
  30. Usacheva, A., Kotenko, S., Witte, M. M., and Colamonici, O. R. (2002) *J. Immunol.* **169**, 1302–1308
  31. Zhou, Y.-J., Chen, M., Cusack, N. A., Kimmel, L. H., Magnuson, K. S., Boyd, J. G., Lin, W., Roberts, J. L., Lengi, A., Buckley, R. H., Geahlen, R. L., Candotti, F., Gadina, M., Changelian, P. S., and O'Shea, J. J. (2001) *Mol. Cell* **8**, 959–969
  32. Schaller, M. D., Otey, C. A., Hildebrand, J. D., and Parsons, J. T. (1995) *J. Cell Biol.* **130**, 1181–1187
  33. Pouillet, P., Gautreau, A., Kadare, G., Girault, J.-A., Louvard, D., and Arpin, M. (2001) *J. Biol. Chem.* **276**, 37686–37691
  34. Chen, R., Kim, O., Li, M., Xiong, X., Guna, J.-L., Kung, H.-J., Chen, H., Shimizu, Y., and Qiu, Y. (2001) *Nat. Cell Biol.* **3**, 439–444
  35. Chen, L.-M., Bailey, D., and Fernandez-Valle, C. (2000) *J. Neurosci.* **20**, 3776–3784
  36. Sieg, D. J., Hauck, C. R., Ilic, D., Klingbeil, C. K., Schaefer, E., Damsky, C. H., and Schlaepfer, D. D. (2000) *Nat. Cell Biol.* **2**, 249–256
  37. Dunty, J. M., and Schaller, M. D. (2002) *J. Biol. Chem.* **277**, 45644–45654
  38. Stewart, A., Ham, C., and Zachary, I. (2002) *Biochem. Biophys. Res. Commun.* **299**, 62–73
  39. Cooper, L. A., Shen, T.-L., and Guan, J.-L. (2003) *Mol. Cell Biol.* **23**, 8030–8041
  40. Dunty, J. M., Gabarra-Niecko, V., King, M. L., Ceccarelli, D. F., Eck, M. J., and Schaller, M. D. (2004) *Mol. Cell Biol.* **24**, 5353–5368
  41. Cohen, L. A., and Guan, J.-L. (2005) *J. Biol. Chem.* **280**, 8197–8207
  42. Jacamo, R. O., and Rozengurt, E. (2005) *Biochem. Biophys. Res. Commun.* **334**, 1299–1304
  43. Pearson, M. A., Reczek, D., Bretschner, A., and Karplus, P. A. (2000) *Cell* **101**, 259–270
  44. Han, B.-G., Numomura, W., Takakuwa, Y., Mohandas, N., and Jap, B. K. (2000) *Nat. Struct. Biol.* **7**, 871–875
  45. Shimizu, T., Seto, A., Maita, N., Hamada, K., Tsukita, S., Tsukita, S., and Hakoshima, T. (2002) *J. Biol. Chem.* **277**, 10332–10336
  46. Kang, B. S., Cooper, D. R., Devedjiev, Y., Derewenda, U., and Derewenda, Z. S. (2002) *Acta Crystallogr. Sect. D Biol. Crystallogr.* **58**, 381–391
  47. Smith, W. J., Nassar, N., Bretschner, A., Cerione, R. A., and Karplus, P. A. (2003) *J. Biol. Chem.* **278**, 4949–4956
  48. Garcia-Alvarez, B., de Pereda, J. M., Calderwood, D. A., Ulmer, T. S., Critchley, D., Campbell, I. D., Ginsberg, M. H., and Liddington, R. C. (2003) *Mol. Cell* **11**, 49–58
  49. Cowtan, K., and Zhang, K. (1999) *Prog. Biophys. Mol. Biol.* **72**, 245–270
  50. Perrakis, A., Morris, R., and Lamzin, V. (1999) *Nat. Struct. Biol.* **6**, 458–463
  51. Laskowski, R. A., MacArthur, M. W., Moss, D. S., and Thornton, J. M. (1993) *J. Appl. Crystallogr.* **26**, 283–291
  52. McCoy, A. J., Grosse-Kunstleve, R. W., Storoni, L. C., and Read, R. J. (2005) *Acta Crystallogr. D Biol. Crystallogr.* **61**, 458–464
  53. Vijay-kumar, S., Bugg, C. E., and Cook, W. J. (1987) *J. Mol. Biol.* **194**, 531–544
  54. Kragelund, B. B., Anderson, K. V., Madsen, J. C., Knudsen, J., and Poulsen, F. M. (1993) *J. Mol. Biol.* **230**, 1260–1277
  55. Blomberg, N., Baraldi, E., Nilges, M., and Saraste, M. (1999) *Trends Biochem. Sci.* **24**, 441–445
  56. Lemmon, M. A., and Keleti, D. (2005) in *Modular Protein Domains* (Cesareni, G., Gimona, M., Sudol, M., and Yaffe, M., eds) pp. 337–357, Wiley, New York
  57. Edwards, S. D., and Keep, N. H. (2001) *Biochemistry* **40**, 7061–7068
  58. Nowakowski, J., Cronin, C. N., McRee, D. E., Knuth, M. W., Nelson, C. G., Pavletich, N. P., Rogers, J., Sang, B.-C., Scheibe, D. N., Swanson, R. V., and Thompson, D. A. (2002) *Structure* **10**, 1659–1667
  59. Prehoda, K. E., Lee, D. J., and Lim, W. A. (1999) *Cell* **97**, 471–480
  60. Tsukita, S., Yonemura, S., and Tsukita, S. (1997) *Trends Biochem. Sci.* **22**, 53–58
  61. Eck, M. J., Dhe-Paganon, S., Trub, T., Nolte, R. T., and Shoelson, S. E. (1996) *Cell* **85**, 695–705
  62. Mitra, S. K., Hanson, D. A., and Schlaepfer, D. D. (2005) *Nat. Rev. Mol. Cell Biol.* **6**, 56–68
  63. Sicheri, F., and Kuriyan, J. (1997) *Curr. Opin. Struct. Biol.* **7**, 777–785

## Crystal Structure of the FERM Domain of Focal Adhesion Kinase

Derek F. J. Ceccarelli, Hyun Kyu Song, Florence Poy, Michael D. Schaller and Michael J. Eck

*J. Biol. Chem.* 2006, 281:252-259.

doi: 10.1074/jbc.M509188200 originally published online October 12, 2005

---

Access the most updated version of this article at doi: [10.1074/jbc.M509188200](https://doi.org/10.1074/jbc.M509188200)

### Alerts:

- [When this article is cited](#)
- [When a correction for this article is posted](#)

[Click here](#) to choose from all of JBC's e-mail alerts

This article cites 62 references, 27 of which can be accessed free at <http://www.jbc.org/content/281/1/252.full.html#ref-list-1>